Improved Lewenstein model for high-order harmonic generation of atoms and molecules with scattering wavefunctions

Anh-Thu Le,[*][1] Toru Morishita,[1,2] and C. D. Lin[1]

[1]*Department of Physics, Cardwell Hall, Kansas State University, Manhattan, KS 66506, USA*
[2]*Department of Applied Physics and Chemistry, University of Electro-Communications,*
1-5-1 Chofu-ga-oka, Chofu-shi, Tokyo, 182-8585, Japan
(Dated: November 2, 2018)

We demonstrate a simple method to improve the Lewenstein model for the description of high-order harmonic generation (HHG). It is shown that HHG spectra can be expressed as the product of a returning electron wave packet and the photo-recombination cross sections, where the former can be extracted from the Lewenstein model. By replacing plane waves with scattering waves in the calculation of recombination matrix elements, we showed that the resulting HHG spectra agree well with those from solving the time-dependent Schrödinger equation. The improved model can be used for quantitative calculations of high harmonics generated by molecules.

When an atom is subjected to a strong driving laser field, one of the nonlinear response processes is the generation of high-order harmonics. In the past decade, high-order harmonic generation (HHG) has been used extensively for the generation of single attosecond pulses [1, 2, 3] and attosecond pulse trains [4], thus opening up new opportunities for attosceond time-resolved spectroscopy. HHG is understood using the three-step model [5, 6] – first the electron is released by tunnel ionization; second, it is accelerated by the oscillating electric field of the laser and later driven back to the target ion; and third, the electron recombines with the ion to emit a high energy photon. A semiclassical formulation of the three-step model based on the strong field approximation (SFA) is given by Lewenstein et al [6]. In this SFA model (often called Lewenstein model), the liberated continuum electron experiences the full effect from the laser field, but not from the ion that it has left behind. In spite of this limitation, Lewenstein model has been widely used for understanding the HHG by atoms and molecules. Since the continuum electron needs to come back to revisit the parent ion in order to emit radiation, the neglect of the electron-ion interaction is rather questionable. Thus, various efforts have been made to improve upon the Lewenstein model, by including Coulomb distortion [7, 8], or by using Ehrenfest theorem [9]. These improvements, however, still do not lead to satisfactory agreement with exact calculations, nor do they reveal how the target affects the HHG spectra.

According to the three-step model, the last step of HHG is the recombination process. Taking this model seriously, one can ask if the HHG yield can be written as the product of a returning electron wave packet with the photo-recombination cross section, and if the electron wave packet is largely independent of the targets. These two assumptions are at the heart of the tomographic procedure of Itatani et al. [10]. Their validity has been established for N_2 and O_2 molecules where the HHG spectra were calculated using the Lewenstein model and the photo-recombination cross sections were calculated using the plane-wave approximation (PWA) [11]. The independence of the returning wave-packet on the atomic rare gas targets has recently been investigated by Levesque et al. [12], where the dipole matrix elements (or recombination cross sections) were also calculated within the PWA.

More recently, using HHG spectra obtained from numerical solutions of the time-dependent Schrödinger equations (TDSE) for atoms in an intense laser field, Morishita et al. [13] showed that the "exact" TDSE results can be expressed as

$$S(\omega) = W(E)\frac{d\sigma(\omega)}{d\Omega_{\boldsymbol{k}}}, \qquad (1)$$

where $d\sigma/d\Omega_{\boldsymbol{k}}$ is the "exact" photo-recombination (differential) cross section. Here W describes the flux of the returning electrons, which we will call a "wave-packet". The electron energy E is related to the emitted photon energy ω by the relation $E = k^2/2 = \omega - I_p$, with I_p being the ionization potential of the target (atomic units are used throughout this paper, unless otherwise indicated). The method for solving the TDSE and the calculation of $d\sigma/d\Omega_{\boldsymbol{k}}$ are described later.

In this Letter, we will first show that if the HHG yield calculated within the Lewenstein model is written as

$$S^{SFA}(\omega) = W^{SFA}(E)\frac{d\sigma^{PW}(\omega)}{d\Omega_{\boldsymbol{k}}}, \qquad (2)$$

then the electron "wave packet" W^{SFA} will be largely identical to W^{TDSE} obtained from Eq. (1) by solving the TDSE in the same laser pulse. Here $d\sigma^{PW}/d\Omega_{\boldsymbol{k}}$ is the recombination cross section calculated the plane wave approximation. In the improved Lewenstein model, or the
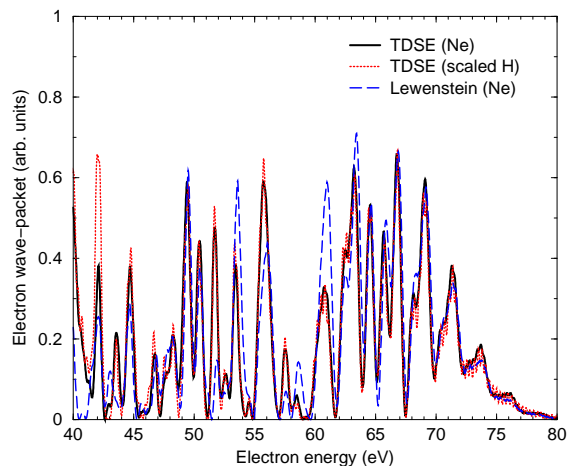
*Email address: atle@phys.ksu.edu

FIG. 1: (Color online) Comparison of the electron "wave packets" extracted from the exact HHG spectra of Ne, obtained by solving the TDSE (solid black line), and from the Lewenstein model (dashed blue line). Also shown is the TDSE result for a scaled H (dotted red line). The laser pulse is with duration of 10.3 fs, peak intensity of 2×10^{14} W/cm^2 and mean wavelength of 1064 nm.

scattering wave based strong-field approximation (SW-SFA), we propose that the HHG be calculated by

$$S^{SW-SFA}(\omega) = W^{SFA}(E)\frac{d\sigma(\omega)}{d\Omega_{\boldsymbol{k}}}. \tag{3}$$

In Fig. 1, we show the wave-packets extracted from the HHG spectra of Ne (solid black line) and from scaled H (dotted red line) by using Eq. (1), where the "exact" HHG spectra are obtained from the solution of the TDSE and the photo-recombination cross sections are calculated with "exact" scattering wavefunctions. The effective nuclear charge of the companion H is chosen such that it has the same 1s binding energy as the Ne(2p) state. We use a laser pulse with duration (FWHM) of 10.3 fs, peak intensity of 2×10^{14} W/cm^2 and mean wavelength of 1064 nm. Clearly, the two wave packets agree very well. Additional evidences of such agreement can be found in our recent work [13], where Eq. (1) was also utilized to extract very accurate photo-recombination cross sections for a variety of atomic targets. The extracted electron wave packet W^{SFA} is shown as the dashed blue line. This result, which has been normalized to that of the TDSE near the cutoff, agrees reasonably well with the TDSE result. We have also performed calculations for different atoms and with different laser parameters to confirm this conclusion.

Having established the good agreement between W^{SFA} and W^{TDSE}, we now present the main results in Fig. 2. Here we show the HHG spectra calculated using the direct solution of the TDSE (solid red lines), Lewenstein model (dotted blue lines), together with the SW-SFA model (solid black lines) for Ar, Xe, and Ne. For Ar
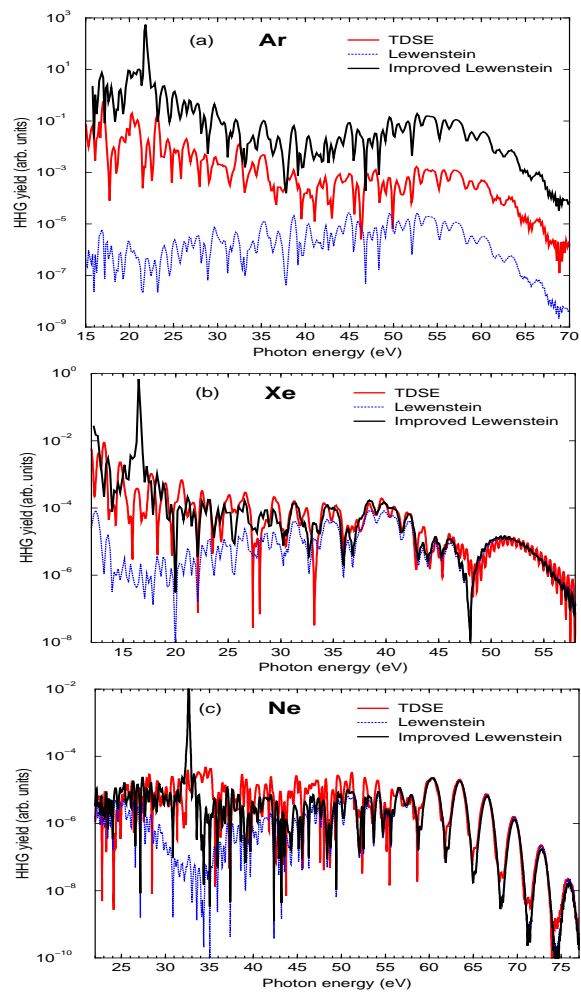

FIG. 2: (Color online) Comparison of the HHG yields obtained from numerical solution of the TDSE (solid red lines), the Lewenstein model (dashed blue lines), and the improved Lewenstein model (solid black lines) for Ar (a), Xe (b), and Ne (c).

and Ne, the laser pulse has peak intensity of 2×10^{14} W/cm^2 and mean wavelength of 800 nm. The laser duration (FWHM) is 10 fs for Ar and 20 fs for Ne. For Xe, the corresponding parameters are 5×10^{13} W/cm^2, 1600nm, and 7.8 fs, respectively. The HHG yields for Ar are shifted vertically in order to show their detailed structures. For Ne and Xe, the SFA and SW-SFA results are normalized to the TDSE results near the cutoff, i.e., close to $3.2U_p + I_p$, where U_p is the ponderomotive energy.

First we compare the SFA and the TDSE results. Clearly, the Lewenstein model agrees reasonably well only in some range near the HHG cutoff for all three cases. For Ar, they agree well for a broad range from 70 eV down to 40 eV. Near 40 eV, the slope of the TDSE curve changes and the two results start to deviate. The discrepancy reaches more than two orders of magnitude near the ionization threshold (15.76 eV). For
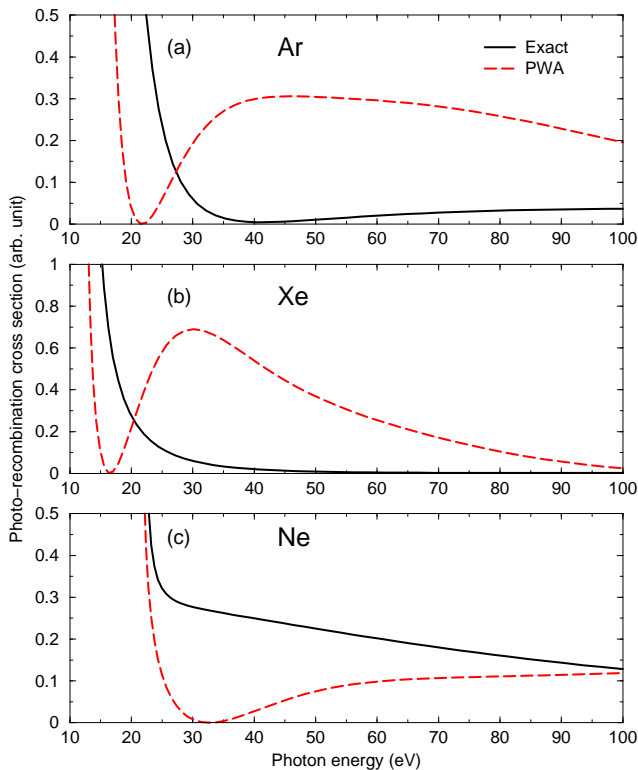
FIG. 3: (Color online) Photo-recombination cross sections of Ar (a), Xe (b) and Ne (c), obtained by using exact scattering wavefunctions (solid curves) and within the plane-wave approximation (dashed curves).

Xe, the Lewenstein model underestimates the HHG yield by up to one or two orders of magnitude, begining just below the cutoff. The inaccuracy of the SFA for lower harmonics is usually interpreted as due to the neglect of the interaction between the target ion and the continuum electron in the three-step model. While this interpretation is qualitatively correct, it does not explain why in some cases the agreement is better. For example, see Fig. 2(c) for Ne. Here the HHG yield from the Lewenstein model disagrees with the TDSE results only in the range from 28 eV to 45 eV.

We next examine the prediction of the SW-SFA model. From Fig. 2 it is clear that it gives much better agreement with the TDSE results for all three atoms shown. In some cases, the discrepancy has been reduced from two orders of magnitude in the SFA to about a factor of two in the SW-SFA. Since the recombination cross sections calculated using "exact" scattering wavefunctions are independent of the electromagnetic gauges used, unlike the SFA, the SW-SFA model has no gauge-dependence issues. There are some "unphysical" sharp spikes in Fig. 2, near 22 eV in Ar, 17 eV in Xe, and 32 eV in Ne. They are due to the "Cooper minima" where the photo-recombination cross sections $d\sigma^{PW}/d\Omega_{\boldsymbol{k}}$ vanish (see Fig. 3).

In order to understand the nature of the improvement

in the SW-SFA, we now analyze the photo-recombination cross sections. In Figs. 3 (a), (b), and (c) we compare the exact results, $d\sigma/d\Omega_{\boldsymbol{k}}$, with $d\sigma^{PW}/d\Omega_{\boldsymbol{k}}$ for Ar, Xe, and Ne, respectively. The figures show that, by approximating scattering waves by plane waves, the calculated dipole matrix elements are quite inadequate for electron energies below 100 eV. In particular, in Ne there is a spurious "Cooper minimum" near 32 eV if the plane wave is used. This minimum is totally absent for the whole energy range in the exact result. The Cooper minima are known to be related to the zeros in the dipole matrix elements and they are absent for Ne since the 2p wavefunction is nodeless [14]. We note, from Fig. 3(b), the position of the Cooper minimum for Ar predicted by using the PWA is shifted lower by about 20 eV as compared to the exact result. For the Xe case, the shift is even larger (the "exact" Cooper minimum, which is near 80 eV, is not clearly seen in Fig. 3(b)).

The theoretical method for the numerical solution of the TDSE has been described previously [15, 16]. The electric field of the laser pulse is written in the form $E(t) = E_0 a(t) \cos(\omega t + \phi)$, with the envelope given by $a(t) = \cos^2(\pi t/\tau)$, where τ is 2.75 times the FWHM of the laser pulse. All the atoms are approximated by a one-electron model potential $V(r)$ which has the form of $V(r) = V_s(r) - 1/r$. The parameters in the model potential are chosen such that the binding energies of the ground state and the first few excited states are close to the experimental values. We then propagate the initial ground state in time using the split operator method. The laser parameters were chosen such that the depletion effect is small. Typically the ground state survival probability is more than about 95%.

Photo-recombination cross section is determined as

$$\frac{d\sigma(\omega)}{d\Omega_{\boldsymbol{k}}} = \frac{\omega^3}{2\pi k} \left| \langle \Psi_{\boldsymbol{k}}^+ | z | \Phi_0 \rangle \right|^2, \qquad (4)$$

where $|\Psi^+\rangle$ and $|\Phi_0\rangle$ are the scattering wavefunction and the ground state wavefuntion, respectively, and $\Omega_{\boldsymbol{k}} \equiv \{\theta_{\boldsymbol{k}}, \phi_{\boldsymbol{k}}\}$ is the direction of $\boldsymbol{k}$. The returning electron that contributes most to the HHG is the one that propagates along the laser polarization direction. Therefore, the relevant cross section is for $\boldsymbol{k}$ that is parallel to z-axis (the laser polarization axis), that is, $\theta_{\boldsymbol{k}} = 0$ or π.

For each model potential $V(r)$, continuum scattering wavefunctions are calculated numerically, using the partial-wave expansion

$$\Psi_{\boldsymbol{k}}^+(\boldsymbol{r}) = \sum_{l=0}^{\infty} i^l e^{i\delta_l} \frac{R_{kl}(r)}{k} \sum_{m=-l}^{l} Y_{lm}^*(\theta_{\boldsymbol{k}}, \phi_{\boldsymbol{k}}) Y_{lm}(\theta, \phi) \quad (5)$$

where $\delta_l(k)$ is the partial-wave phase shift. With this scattering wave function, "exact" photo-recombination cross section is then obtained by using Eq. 4. Note that for atoms which have p_0 ground states, only $l = 0, 2$ and $m = 0$ will contribute to the dipole matrix element. It
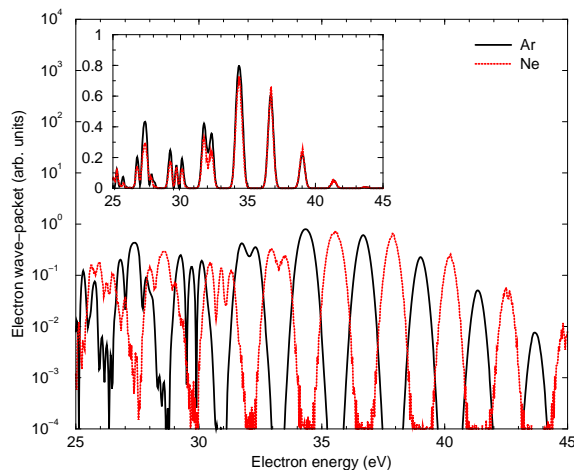
FIG. 4: (Color online) The electron wave-packets, extracted from the HHG spectra for Ne and Ar under the same laser field. The inset shows the wave-packets in the linear scale with the Ne data shifted horizontally by -1.2 eV. The HHG are obtained within the Lewenstein model with 1064 nm laser, peak intensity of 2×10^{14} W/cm^2, duration of 50 fs.

is interesting to note that for all the systems considered here, the shape of $d\sigma/d\Omega_{\boldsymbol{k}}$ as functions of photon energy are quite close to the total (integrated) cross sections, obtained by averaging over $m = -1, 0, 1$ initial states. In the PWA, a plane-wave $(2\pi)^{-3/2} \exp(\imath \boldsymbol{kr})$ is used to obtain $d\sigma^{PW}/d\Omega_{\boldsymbol{k}}$.

So far we have extracted photo-recombination cross sections from Ar, Xe, and Ne by using companion atoms with nearly identical ionization potentials, as compared to the atoms under consideration [13]. This is used to greatly simplify the analysis. In the following, we will show that this requirement can be relaxed. As the wave packets obtained within the Lewenstein model agree reasonably well with the TDSE results, for our purpose we only use the Lewenstein model in the subsequent analysis. In Fig. 4, we show the comparison of the wave packet from Ne ($I_p = 21.56$ eV) and Ar ($I_p = 15.76$ eV) in the same 1064 nm laser pulse with peak intensity of 2×10^{14} W/cm^2, duration (FWHM) of 50 fs. Clearly, the two wave packets lie nicely within a common envelope. This can be seen even more clearly in the inset, where the data are plotted in linear scale with the Ne data shifted horizontally by -1.2 eV. We note that the small details below 33 eV also agree well. This conclusion is also confirmed by our calculations using the TDSE with different laser parameters and with other atoms. This supports that the independence of the wave packet on the target structure can also be extended to systems with different ionization potentials.

In this Letter, we have shown that the improved Lewenstein model is capable of describing HHG spectra close to the accuracy that can only be achieved by solving the TDSE directly. Extending this model to

molecules, we expect that accurate HHG spectra from molecular targets can be calculated. For molecules, accurate solutions of the TDSE are very time-consuming, if not impossible. Using the Lewenstein model, the HHG as well as the dipole matrix elements can be easily calculated [17, 18] to extract the wave packet. Similarly, theoretical tools for the calculation of molecular photo-recombination (or photoionization) cross sections are quite mature, and general computer codes are available even for large molecules [19]. Thus it is expected that HHG spectra generated by molecules can be calculated using the SW-SFA model readily. Finally, we mention that the present analysis has not yet addressed the phases of the harmonics. Further studies would be needed to disentangle the phases due to the laser and the target separately. This step is needed in order to incorporate propagation effect of the medium on the generated high harmonics.

[1] M. Drescher et al., Nature (London) **419**, 803 (2002).
[2] T. Sekikawa et al., Nature (London) **432**, 605 (2004).
[3] G. Sansone et al., Science **314**, 443 (2006).
[4] R. Lopez-Martens et al., Phys. Rev. Lett. **94**, 033001 (2005).
[5] P. B. Corkum, Phys. Rev. Lett.**71**, 1994 (1993).
[6] M. Lewenstein et al., Phys. Rev. A **49**, 2117 (1994).
[7] M. Yu. Ivanov, T. Brabec, and N. Burnett, Phys. Rev. A **54**, 742 (1996).
[8] J. Z. Kaminski and F. Ehlotzky, Phys. Rev. A , **54**, 3678 (1996).
[9] A. Gordon and F. X. Kärtner, Phys. Rev. Lett. **95**, 223901 (2005).
[10] J. Itatani et al., Nature **432**, 867 (2004).
[11] V. H. Le, et al., Phys. Rev. A., **76**, 013414 (2007).
[12] J. Levesque et al., Phys. Rev. Lett. **98**, 183903 (2007).
[13] T. Morishita, A. T. Le, Z. Chen, and C. D. Lin, arXiv:0707.3157v1 [physics.atom-ph] (submitted to Phys. Rev. Lett.).
[14] A. F. Starace, Theory of atomic photoionization, Springer Verlag, Berlin (1982).
[15] Z. Chen et al., Phys. Rev. A **74**, 053405 (2006).
[16] T. Morishita et al., Phys. Rev. A **75**, 023407 (2007).
[17] X. X. Zhou et al., Phys. Rev. A **71**, 061801(R) (2005).
[18] A. T. Le et al., Phys. Rev. A **73**, 041402(R) (2006).
[19] S. Tonzani, Comput. Phys. Comm. **176**, 146 (2007).